# Controlled Deployment of Gossamer Spacecraft

By Patric SEEFELDT, Tom SPROEWITZ, Peter SPIETZ, Eugen MIKULZ, Siebo REERSHEMIUS, Kaname SASAKI, Norbert TÓTH and Rico JAHNKE

*Institute of Space Systems, German Aerospace Center (DLR), Bremen, Germany*

Deployable gossamer structures for solar sails need to be deployed in a controlled way. Several strategies present have the disadvantage that the sail membrane cannot always be tensioned during the deployment process. In combination with a slow deployment, this involves the risk of an entanglement of the sail. Slow deployments of at least several minutes are desirable in order to keep inertial loads low and to implement Fault-Detection, Fault-Isolation and Recovery Techniques (FDIR). This might further require completely stopping and resuming the deployment process.
For gossamer spacecraft based on crossed boom configurations with triangular sail segments, a deployment strategy is described that is assumed to allow such a controlled deployment process.
With a combination of folding and coiling, it is ensured that the deployed sail area can be held taut between the partly deployed booms. During deployment, four deployment units with two spools each on which the sail is mounted (a half segment stowed on each) moves away from the central bus unit, the center of the deployed sail. The development was made in the Gossamer-1 project of the German Aerospace Center (DLR).
The folding and coiling of the membrane is mathematically modelled. This allows an investigation of the deployment geometry. It provides the mathematical relation between the deployed boom length and the deployed sail membrane geometry. By modelling the coiled zig-zag folding lines it is possible to calculate the deployment force vector as function of the deployment time.
The stowing and deployment strategy was verified by tests with an engineering qualification model of the Gossamer-1 deployment unit. According to a test-as-you-fly approach the tests included vibration tests, venting, thermal-vacuum tests and ambient deployment. In these tests the deployment strategy proved to be suitable for a controlled deployment of gossamer spacecraft. A deeper understanding of the deployment process is gained by analyzing the deployment strategy mathematically.

**Key Words: Deployment Systems, Deployment Strategy, Controlled Deployment**

## Nomenclature

| | | |
|---|---|---|
| $C$ | : | cathetus |
| $F$ | : | force |
| $H$ | : | hypotenuse |
| $K$ | : | integration constant |
| $l$ | : | length |
| $m$ | : | spiral slope |
| $n$ | : | number of |
| $r$ | : | radius |
| t | : | thickness |
| w | : | width of folded sail |
| $x$ | : | Cartesian coordinate |
| $y$ | : | Cartesian coordinate |
| $z$ | : | Cartesian coordinate |
| $\alpha$ | : | sail spool rotation angle |

Subscripts

| | | |
|---|---|---|
| D | : | deployment |
| c | : | cathetus |
| f | : | folded segment |
| h | : | hypotenuse |
| i | : | inner |
| s | : | sail spool |

## 1. Introduction

Studies investigating how to stow membranes for space applications go back to the 1980s. Miura [1] already stated general requirements for the packaging of membranes for space applications. He described that folding and deployment are two phases of a reversible process. Reversible means, that the chosen stowing strategy must allow an autonomous deployment in space. It should be supplemented that the stowed sail needs to withstand all launch loads, namely shock, vibrations and fast decompression. Such a qualification process is described in [2].

With respect to the differentiation of folding strategies, Miura [1] distinguished one-dimensional and two-dimensional folding techniques. The differentiation is made by the in-plane dimensions of the membrane that shrink due to the folding process. Due to the size of the membranes considered, it is of course always necessary to reduce both dimensions. This can be achieved by combining two one-dimensional folding processes or by employing an additional coiling of the previously folded membrane. An overview of frequently considered stowing strategies is given in Fig. 1. Guest [3] describes patterns allowing the wrapping of a membrane around a central hub, and De Focatiis [4] presents different folding patterns based on the folding of tree leaves. Double zig-zag folding patterns, sometimes referred to as frog-leg folding, were employed, for example, by Leipold [5] and

Stohlman [6]. A combined folding and central coiling of a sail membrane split into four triangular segments was implemented for JAXA's IKAROS sail [7] and for a Cubesat and on a CubeSat level this is presented in [8].

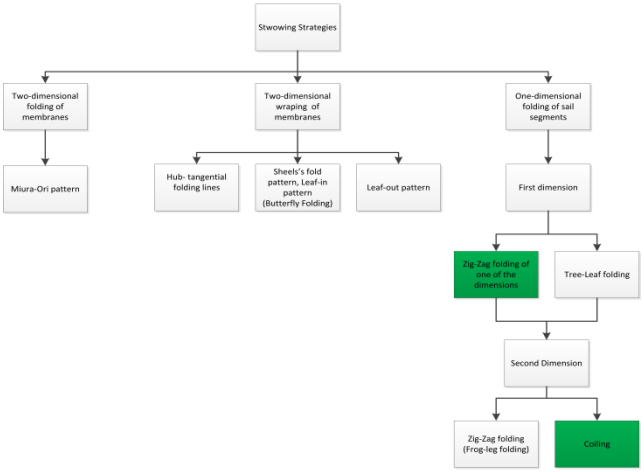


Fig. 1. Overview of frequently considered stowing and deployment strategies overview. The strategy considered here is based on the green highlighted combination.

In the last several years, the further development of scalable deployment technology for gossamer spacecraft systems, suitable for autonomous and controlled deployment was pursued at the German Aerospace Center (DLR) in the Gossamer-1 project. An overview of the technology and the mission behind it is presented in [9]. The aim of the project was to develop a deployment system for space applications with a focus on solar sailing and secondary use cases as a flexible photovoltaic array and drag sail. The development was carried out for a 5 m x 5 m technology demonstrator that should in principal allow for up-scaling to 50 m x 50 m. The sail is based on a crossed boom configuration with four triangular sail segments.

Pursuing the goal of having a controllable configuration during the deployment, the main difference with the Gossamer-1 deployment strategy is that the membrane is stowed on four deployment units that, during deployment, move away from the central unit (the center of the deployed sail). Fig. 2 illustrates the deployment process. By uncoiling the booms, the deployment units move outwards, thereby deploying the sail segments simultaneously. After the sail deployment is completed, the sail segments are separated from the deployment mechanism and the deployment units are jettisoned.

In the following sections the Gossamer-1 stowing and deployment strategy is analyzed. It is assumed that during deployment the strategy always provides a controllable and mechanically stable configuration. In Section 2, this aspect and other design drivers are pointed out. This is followed by an introduction of a mathematical description of the deployment geometry. Section 3 gives an overview of resent verification testing and Section 4 provides a conclusion.

## 2. Stowing strategy

One of the first considerations for a stowing technique was that rectangular, not-folded areas for the photovoltaics were needed. Additionally, the photovoltaic strings were mounted such that they were lying face to face on top of each other. This resulted from electrical insulating considerations. Therefore, the specific peculiarities of the photovoltaics alone already caused the consideration of a combined folding and coiling strategy.

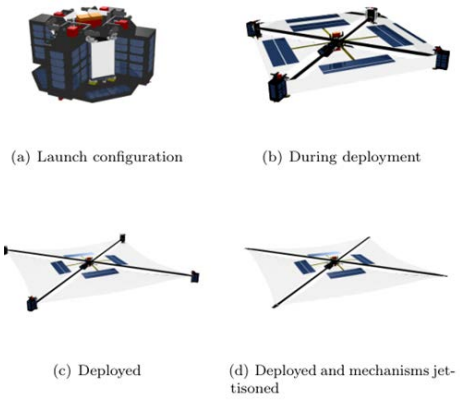


Fig. 2. Gossamer-1 deployment sequence

In a first attempt, the sail deployment mechanism was supposed to be part of the central spacecraft unit. Therefore the stowing strategy shown in Fig. 3 was chosen, where each sail segment was coiled on one spool.

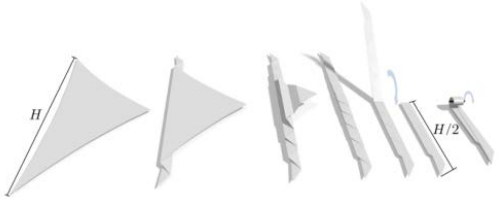


Fig. 3. First idea for a sail stowing strategy with deployment mechanisms mounted on the central spacecraft unit.

While a derivation of this strategy, for which all folded segments were coiled on one spool, was successfully employed for a CubeSat sail (see [8]), it was not compliant with the requirement of a controlled deployment. The folded sail segments have a length of $H/2$, where $H$ is the hypotenuse of the sail segment. When the booms are deployed to this length, the complete sail segment slides off of the spool. One can observe this behavior during the deployment of a 2 $m^2$ sail on a REXUS sounding rocket shown in Fig. 4. The two small pictures in the second row show the booms not yet fully deployed but with the complete sail segments already off the spool and not tensioned. What is not a problem with a small 2 $m^2$ sail in a highly dynamic deployment process (deployment time less than a second) becomes difficult to handle with a sail off several tenths or even hundredths of square-meters deployed in about 20 to 30 minutes or even longer. This obvious disadvantage let to a rethinking of the stowing and deployment technique.

Taking that under the given geometric constraints (e.g. crossed booms) triangular sail segments are chosen, it is apparently necessary to deploy the full length of the hypotenuse at the end of the deployment process. This led to a strategy which coils the folded sail segments onto two spools, starting from the outer edges (see Fig. 5). The triangular segments are first zig-zag folded and then coiled onto two spools. The spools are mounted on two neighboring deployment units (see Fig. 2a).

### 2.1. Mathematical model of the stowing and deployment geometry

For the analysis, a paper model scaled 1:30 of one sail segment was made, as shown in Fig. 5. The figure also provides the symbols used and coordinate systems.

When implementer the zig-zag folding, the result is a sail stripe with $n_f$ folding lines and $n_f + 1$ layers of foil. The hypotenuse is coiled on the spool, together with all other layers of the folded sail to a spiral like geometry as

$$l_{h_{coiled}} = \begin{pmatrix} l_{h,x_s} \\ l_{h,y_s} \end{pmatrix} = \begin{pmatrix} r(\alpha) \cdot cos(\alpha) \\ r(\alpha) \cdot sin(\alpha) \end{pmatrix} \tag{1.}$$

The cathetus translates into a zig-zag line running up and down along width $w$ of the folded sail segment with the pitch angle $\phi$ The slope $\tan(\phi)$ in the case presented here is one because the sail segment represents a rectangular isosceles triangle. The alternating point appears at $y_f$=0 and $y_f$=$w$ in a $x$-distance of every $w$ (rectangular isosceles triangle).The function of this zig-zag line may be described as

$$l_c(x_f) = \frac{w}{\pi} \cdot cos^{-1}\left[cos\left(\frac{2 \cdot \pi}{2 \cdot w} \cdot x_f\right)\right] \tag{2.}$$

When coiling this sail stripe, the zig-zag line segments translate into a helix which alternates up and down along the sail coil height or the width $w$, respectively. A helix with varying radius $r$ and an alternating slope is described by

$$l_{c_{coiled}} = \begin{pmatrix} l_{c,x_s} \\ l_{c,y_s} \\ l_{c,z_s} \end{pmatrix} = \begin{pmatrix} r(\alpha) \cdot cos(\alpha) \\ r(\alpha) \cdot sin(\alpha) \\ l_{c,z_s}(\alpha) \end{pmatrix}. \tag{3.}$$

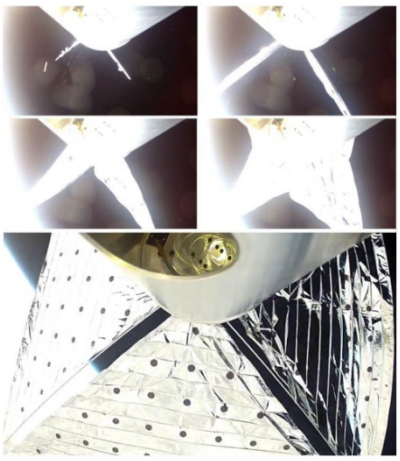

Fig. 4. Deployment of the Space Sailors drag sail on a REXUS sounding rocket.

When summarizing the volume of the material itself it is found that the material coiled on the spool would ideally occupy a volume of $1.436 \cdot 10^{-4}\ \mathrm{m}^3$. When coiling the sail on the spool with an inner radius of 17.5 mm, it is found that the outer radius is about 30 mm. With a folding width of 230 mm this equals a volume coiled on two spools of $8.576 \cdot 10^{-4}\ \mathrm{m}^3$. Due to the sail segment that is not fully compressed, the real volume is about six times bigger than the theoretical one.

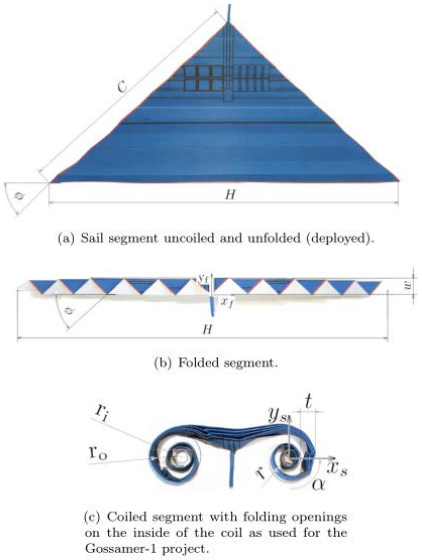


(a) Sail segment uncoiled and unfolded (deployed).

(b) Folded segment.

(c) Coiled segment with folding openings on the inside of the coil as used for the Gossamer-1 project.

Fig. 5. Paper model of a sail segment, scale 1:30 with symbols for the basic dimensions.

The mathematical model of the thickness of folded segment $t$ can be simplified into a linear variation with slope $m$ as

$$\frac{dt}{d\left(\frac{H}{2} - x_f\right)} = m \tag{4.}$$

When coiling the folded sail segment onto a spool, the thickness of the folded sail segment translates into a change of radius and $x_f$ translates into an arc length:

$$\frac{dt}{d\left(\frac{H}{2} - x_f\right)} = \frac{dr}{rd\alpha} = m \tag{5.}$$

This is by definition a logarithmic spiral. By separation of variables and integration the function of the radius is achieved, which is

$$r(\alpha) = K \cdot e^{\pm m \cdot \alpha}. \tag{6.}$$

The sign of $m \cdot \alpha$ indicates the coiling direction which differs for the two spools used for the coiling. The constant $K$ is determined so that the inner spool radius $r_i$ is achieved at $\alpha = 0$. If it would be taken very exactly, one would have to differentiate between the first rotation on the circular spool and the next rotations where the layers are coiled on each other. It should be noted that a detailed modeling of the function has a negligible impact on the further results presented here. This is because the spiral needs a correction factor $c$ that takes the actually achieved stowing volume into

account that is significantly bigger than the pure material volume. The spiral is thereby described as

$$r(\alpha) = r_i \cdot e^{\pm m \cdot c \cdot \alpha} \,. \tag{7.}$$

Taking Equation 6 into account, the function of the zig-zag line according to Equation 3 can be described as the function of the coiling angle $\alpha$ by taking into account that

$$d\left(\frac{H}{2} - x_f\right) = r \cdot d\alpha, \tag{8.}$$

and thereby

$$\begin{aligned} \frac{H}{2} - x_f &= \int_0^{\alpha} r(\alpha)\, d\alpha \\ &= \pm \frac{r_i}{m \cdot c} \cdot \left(e^{\pm m \cdot c \cdot \alpha} - 1\right) \\ \Leftrightarrow x_f &= \frac{H}{2} \mp \frac{r_i}{m \cdot c} \cdot \left(e^{\pm m \cdot c \cdot \alpha} - 1\right) \,. \end{aligned} \tag{9.}$$

The zig-zag line as a function of coiling angle $\alpha$ is achieved by replacing variable $x_f$ in Equation 3 accordingly as

$$\begin{aligned} l_{c,z_s}(\alpha) = \frac{w}{\pi} \cdot cos^{-1}\Big\{cos\Big[\frac{\pi \cdot H}{w \cdot 2} \\ \mp \frac{\pi \cdot r_i}{w \cdot m \cdot c} \cdot \left(e^{\pm m \cdot c \cdot \alpha} - 1\right)\Big]\Big\} - \frac{w}{2} \,. \end{aligned} \tag{10.}$$

With Equations 8 and 11 the folded and coiled cathetus of the sail segment is described by the helix with alternating slope according to Equation 4.

The uncoiled length during the deployment can be described by the arc length of Equations 2 and 4 as

$$\begin{aligned} |l_c| &= \int_{\alpha_{max}}^{\alpha} \left[\left(\frac{\mathrm{dl_{c,x_s}}}{\mathrm{d}\alpha}\right)^2 + \left(\frac{\mathrm{dl_{c,y_s}}}{\mathrm{d}\alpha}\right)^2 + \left(\frac{\mathrm{dl_{c,z_s}}}{\mathrm{d}\alpha}\right)^2\right]^{\frac{1}{2}} \mathrm{d}\alpha \\ &= \frac{r_i \cdot \sqrt{2 + (m \cdot c)^2}}{m \cdot c} \cdot \left(e^{m \cdot c \cdot \alpha} - e^{m \cdot c \cdot \alpha_{max}}\right) \end{aligned} \tag{11.}$$

and

$$\begin{aligned} |l_h| &= \int_{\alpha_{max}}^{\alpha} \left[\left(\frac{\mathrm{dl_{h,x_s}}}{\mathrm{d}\alpha}\right)^2 + \left(\frac{\mathrm{dl_{h,y_s}}}{\mathrm{d}\alpha}\right)^2\right]^{\frac{1}{2}} \mathrm{d}\alpha \\ &= \frac{r_i \cdot \sqrt{1 + (m \cdot c)^2}}{m \cdot c} \cdot \left(e^{m \cdot c \cdot \alpha} - e^{m \cdot c \cdot \alpha_{max}}\right) \,. \end{aligned} \tag{12.}$$

By analyzing the deployment geometry and the deployment force introduced by the mechanism the deployment forces (see Fig. ) and its progression can be analyzed. Such an analysis is currently under review at advances in space research.

## 3. Verification Testing

According to the design presented in [9] an engineering qualification model (EQM) of the deployment unit was built that could be subjected to first environmental tests. It was subjected to a complete test cycle including mechanical vibration testing, venting, thermal-vacuum cycles and ambient deployment (in this order). The EQM included all mechanisms, electronics, two sail segments and one boom. Due to funding reasons it did not include a battery and operational photovoltaic arrays on the deployment unit walls. Instead mass dummies for these components were used and the power supply came through the EGSE plug on the backside of the deployment unit. The EQM was mounted on a test adapter using the hold down and release mechanisms as presented in [9]. The adjacent sail spools that would be mounted on the other deployment units were mounted on this test adapter in the representative way. The EQM mounted on the test adapter just before testing is shown in Fig. 5.

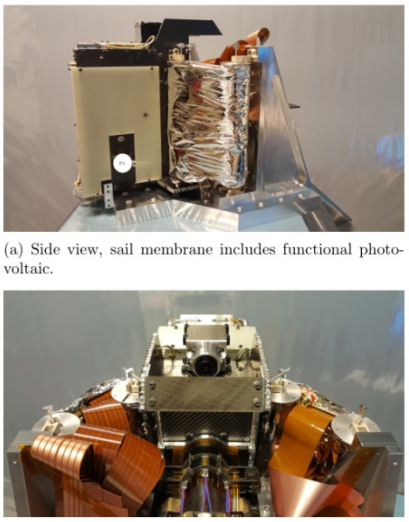

(a) Side view, sail membrane includes functional photovoltaic.

(c) Front view (from CSCU).

Fig. 5. Engineering-qualification model of the Gossamer-1 deployment unit with one boom and two sail segments

### 3.1. Vibration Test

When testing folded and coiled foils it is not possible to put acceleration sensors directly on the foil. The mass of the sensor itself would obviously significantly influence the behavior of the foil. By that reasoning, the acceleration sensors were only put on solid structures such as the sail spool itself. These sensors give an impression of the loads transferred to the folded and coiled sail segment. Fig. 6 shows the response of the sail spool on the sinusoidal loads and Fig. 7 shows the response to the random loads.

The stowed sail as well as the complete EQM passed the vibration test without any visible damage and was then subjected to a venting test. The test was part of a complete verification of the deployment system and the loads were relatively low. On component level the stowed sail was already exposed to much higher loads [2].

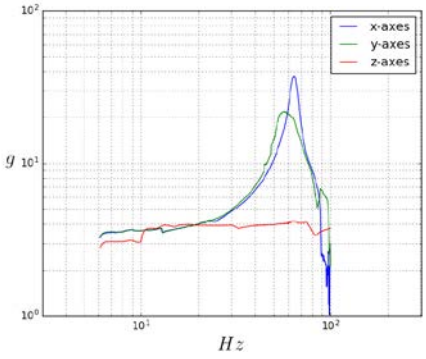


Fig. 6. Response to sinusoidal loads measured on the sail spool.

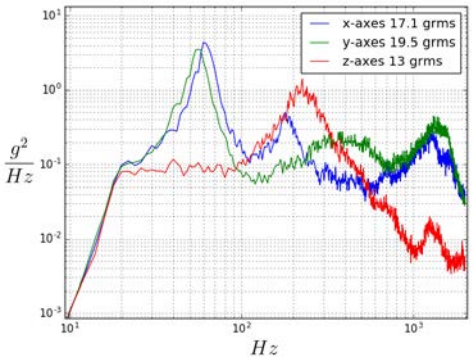


Fig. 7. Response to random loads measured on the sail spool.

### 3.2. Venting Test

The venting test is made by interconnecting a small venting chamber (0.7 $m^3$) to a big vacuum chamber (17 $m^3$) with a valve (see Fig. 8). The Gossamer-1 project had to deal with uncertainties regarding possible launch vehicles, included modified military missiles. The pressure decrease chosen for the venting test as shown in Fig. 9 was therefore much stronger then what would be expected for conventional launch vehicles like the VEGA or Ariane 5 launcher (see launcher manuals).

Fig. 8. Venting test setup.

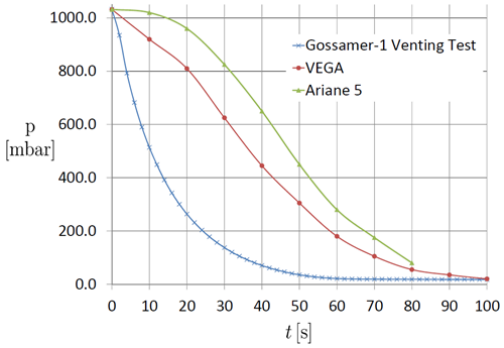


Fig. 9. Pressure during venting test and comparison to VEGA and Ariane 5 launcher (see launcher manual).

### 3.3. Thermal Cycling

In a first thermal-vacuum test cycles between roughly +50°C and -40°C were tested. The test setup is presented in Fig. 10 and the temperature progression is shown in Fig. 11. The BSDU was still mounted on the test adapter but in addition a board with rolls was mounted underneath it. On every hot and cold plateau a functional check of the electronics was made and the motor was activated but not rotated. Actual thermal-vacuum deployment was not made. After the thermal cycling the hold down and release mechanisms were activated and the separation of the BSDU was executed. During the separation the BSDU rolled a few centimeters on the board.

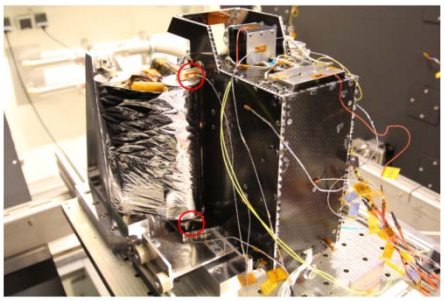

Fig. 10. Test setup for thermal vacuum test.

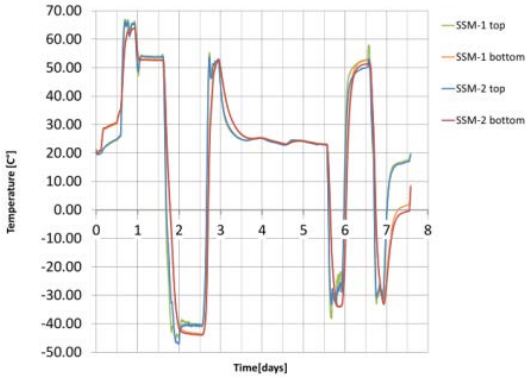


Fig. 11.Thermal vacuum temperature cycles.

The functional check-out of the electronics worked well and also the motor always responded. The hold down and release mechanisms all worked, but the safety cap of the frangibolt was not sufficiently sized and destroyed by the cracking bolt. The separation after the thermal cycling also worked smoothly. The deployment was afterward continued on a deployment test rig.

### 3.4. Ambient Deployment

For the deployment test the same test-setup as used for the engineering model was used (see [9]). The two deployed segments are shown in Fig. 12 and the force measured during deployment on one of the sail spools are shown in Fig. 13.

The total deployment force measured was most of the time between 2N and 3N, only when tensioning the sail against gravity loads at the end of the deployment these forces are increasing. The load was mainly directed along the boom axis. The fast oscillations present are due to the used brake mechanism for the sail spool (see [9]). At time $t_1$ and $t_2$ the deployment was interrupted in order to perform system checks. At time *t3* the support for the photovoltaic area of the sail started to carry gravity load and at $t_4$ the photovoltaic area was fully supported. At $t_5$ additional support for the sail started to carry gravity loads ant at $t_6$ the sail was fully supported and then further tensioned until $t_7$.

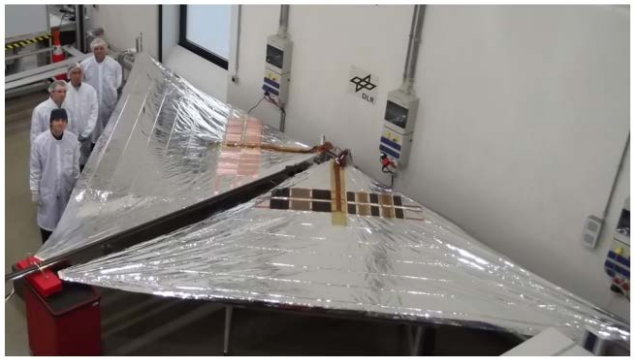

Fig. 12. Two sail segment deployed by the EQM of the deployment unit after the deployment test.

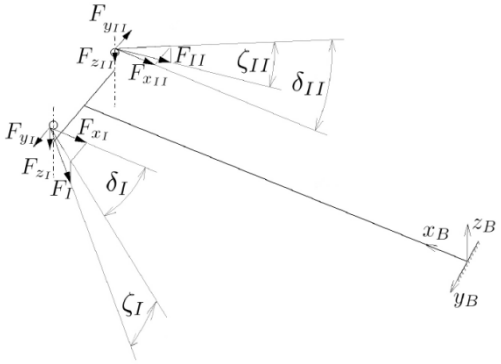


Fig.13. Geometry of the forces applied through the membrane to the spool for uncoiling the membrane. The boom is deployed along $x_B$.

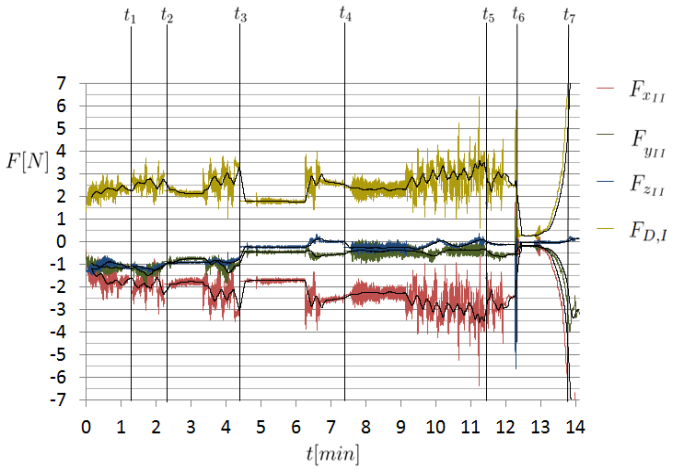


Fig. 14. Measured deployment forces.

## 4. Conclusion

A deployment strategy was invented for a mission that aims to demonstrate a controlled and autonomous deployment in LEO. The deployment geometry is mathematically described and an engineering-qualification model of the deployment unit was tested. A more detailed description of the deployment geometry and forces was recently submitted to Advances in Space Research [10].

Deployment on system level was successfully demonstrated to be controllable, and at no time at risk of entangling. The latter is guaranteed by the folding concept, which ensures that at each stage of deployment, only a minimum amount of the sail is released. The functionality of all mechanisms and electronics was demonstrated.

The deployment technology is between TRL four and five. Actually achieving five would require additional tests (e.g. thermal vacuum deployment) and an increase of robustness of some parts. In addition the integration process needs to be enhanced. These are lessons learned from the test campaign described above.

## References


1) Miura K.: *Method of packaging and deployment of large membranes in space*, Proceedings of the 31st Congress International Astronautical Federation, 1985
2) Seefeldt, P., Steindorf, L. and Spröwitz, T.: *Solar Sail Membrane Testing and Design Considerations*, Proceedings of the European Conference on Spacecraft Structures, Materials & Environmental Testing, 2014.
3) Guest, S. D., and Pellegrino, S: *Inextensional wrapping of flat membranes*, Proceedings of the First International Seminar on Structural Morphology (pp. 203-215), 1992.
4) De Focatiis, D. S. A., & Guest, S. D.: *Deployable membranes designed from folding tree leaves*, Philosophical Transactions of the Royal Society of London A: Mathematical, Physical and Engineering Sciences, 360(1791), 227-238, 2002.
5) Leipold, M., Eiden, M., Garner, C. E. et al.: *Solar sail technology development and demonstration*, Acta Astronautica, 52(2), 317-326, 2003.
6) Stohlman, O. R., Fernandez, J., Lappas, V. J. et al., *Testing of the Deorbitsail drag sail subsystem*, Proceedings of the 54 AIAA/ASME/ASCE/AHS/ASC Structures, Structural Dynamics, and Materials Conference, 2013
7) Tsuda, Y., Mori, O., Funase, R. et al.: *Achievement of IKAROS-Japanese deep space solar sail demonstration mission*, Acta Astronautica, 82(2), 183-188, 2013
8) Wolff, N., Seefeldt, P., Bauer et al.: *Alternative application of solar sail technology*, Advances in Solar Sailing (pp. 351-365), Springer Berlin Heidelberg, 2014.
9) Seefeldt, P., Spietz, P., Sproewitz et al.: *Gossamer-1: Mission Concept and Technology for a Controlled Deployment of Gossamer Spacecraft*, Advances in Space Research, 2016
10) Seefeldt, P.: *A stowing and deployment strategy for large membrane space systems on the example of Gossamer-1*, Submitted to Advances in Space Research, December 23rd 2016